'95 KACC (1995. 10. 23 ~ 25)

Hybrid Impedance Control for Free and Contact Motion

°Yonghwan Oh*, W. K. Chung** and Y. Youm**

**Professor, School of Mech. Eng., Pohang University of Science & Technology(POSTECH)

*Graduate student, School of Mech. Eng., Pohang University of Science & Technology(POSTECH)

Tel: +82-562-279-2844; Fax: +82-562-279-5899; E-mail:oyh@risbot.rist.re.kr

Abstracts A general task execution with hybrid impedance control method is addressed. The target impedance is expressed in the constraint frame. For the computational simplicity and the robustness improvement, disturbance observer scheme is used. To make stable contact with the environment, the large value of desired inertia gain for the force-controlled subspace is suggested. Numerical examples are given to show the performance of the proposed controller.

Keywords Constraint frame, Hybrid impedance control(HIC), Impact control, Disturbance observer, Q–filter

1. INTRODUCTION

When a manipulator makes contact with the environment, control of both force and motion is required. And also, rebounce due to the impact which is an inevitable phenomena during the transition from free to constrained motion and successive collisions should be avoided. To cope with such situations, two approaches are popular in the robotic field, hybrid control[10] and impedance control[2]. And as an unifying method, combining the advantages of hybrid control and impedance control, hybrid impedance control scheme was proposed[1]. Liu[4] showed some experimental results of hybrid impedance controller and performance of contact motion. For the robustness improvement, PI compensation method is suggested.

Most common approaches[1, 2, 10] can be considered as the nonlinear decoupling and inverse dynamic control method based on exact model of the manipulator. However, these methods require heavy computation efforts for real time control and the performance is sensitive to the parameter variations. To avoid this problem, the disturbance observer technique[6, 3] has been developed recently as a robust control scheme. In the disturbance observer, we can reshape the dynamics of manipulator as that of the nominal model.

In this work, a more convenient form of hybrid impedance control method is derived for real implementation. The target impedance is expressed in the constraint frame and for the computational simplicity and the robustness enhencement, a disturbance observer is employed. Also, an approach to make stable contact with the environment is proposed.

Hereafter, the task space dimension, $m = 3$; Σ^0, Σ^c are reference and constraint frames, respectively; I is identity matrix; the superscript c denotes the quantity expressed in Σ^c; $(\cdot)^T$ means transpose of $(\cdot)$. For the simplicity, we assume the point contact without friction and the local deformation is allowed at the contact point due to the compliance of the environment.

2. EQUATIONS OF MOTION IN CONSTRAINT FRAME

End-effector constraints can be caused by tasks such as tracing a curved surface while pressing it by the end-effector as shown in Fig. 1. For motion and force control of the end-effector, it is more convenient to express the dynamics of manipulator in the constraint frame because position and force controlled spaces should be identified depending on task geometries.

2.1 Description of Constraint Frame

Consider the constraint surface described by

$$\phi(\boldsymbol{x}) = 0. \tag{1}$$

Due to the local deformation, velocity of the end-effector pointing into the constraint surface is nonzero. The unit normal vector of the constraint surface at $\boldsymbol{x}$ can be obtained by

$$\hat{\boldsymbol{n}} = \nabla\phi(\boldsymbol{x})/\|\nabla\phi(\boldsymbol{x})\|. \tag{2}$$

At the contact point, if the desired velocity trajectory $\dot{\boldsymbol{x}}_d(t)$ is given in Σ^0 as shown in Fig. 2, then the unit normal vector $\hat{\boldsymbol{n}}$ and $\dot{\boldsymbol{x}}_d(t)$ span the local plane denoted by $\omega(\boldsymbol{x})$. Let us define an unit vector $\hat{\boldsymbol{t}}_2 \in \Re^3$ as one of tangential components as follows

$$\hat{\boldsymbol{t}}_2 = \hat{\boldsymbol{n}} \times \dot{\boldsymbol{x}}_d/\|\hat{\boldsymbol{n}} \times \dot{\boldsymbol{x}}_d\|. \tag{3}$$

The other unit vector $\hat{\boldsymbol{t}}_1 \in \Re^3$ can be evaluated from

$$\hat{\boldsymbol{t}}_1 = \hat{\boldsymbol{t}}_2 \times \hat{\boldsymbol{n}}. \tag{4}$$

A constraint frame Σ^c can be defined at the point of contact with these unit vectors as bases. A transformation matrix from the reference frame to the constraint frame $\boldsymbol{R}(\boldsymbol{x}) \in \Re^{3\times3}$ is given by

$$\boldsymbol{R} \triangleq \begin{bmatrix} \hat{\boldsymbol{t}}_1 & \hat{\boldsymbol{t}}_2 & \hat{\boldsymbol{n}} \end{bmatrix}^T \tag{5}$$

and $\boldsymbol{R}\boldsymbol{R}^T = \boldsymbol{R}^T\boldsymbol{R} = \boldsymbol{I}$.

2.2 Dynamic Equations of Motion

The relation between $\boldsymbol{\Sigma}^0$ and $\boldsymbol{\Sigma}^c$ is

$$\dot{\boldsymbol{r}} = \boldsymbol{R}\dot{\boldsymbol{x}} = \boldsymbol{R}\boldsymbol{J}\dot{\boldsymbol{q}} = \boldsymbol{J}_c\dot{\boldsymbol{q}} \quad (6)$$

$$\boldsymbol{f}^c = \boldsymbol{R}\boldsymbol{f} \quad (7)$$

where $\dot{\boldsymbol{r}}$ is the end-effector velocity expressed in $\boldsymbol{\Sigma}^c$ and $\boldsymbol{J}_c(\boldsymbol{q}) \triangleq \boldsymbol{R}\boldsymbol{J}(\boldsymbol{q})$. Differentiating (6),we obtain the following equation.

$$\ddot{\boldsymbol{r}} = \boldsymbol{J}_c\ddot{\boldsymbol{q}} + \dot{\boldsymbol{J}}_c\dot{\boldsymbol{q}}. \quad (8)$$

Using (8) and $\boldsymbol{\tau} = \boldsymbol{J}_c^T\boldsymbol{f}_c^c$, equations of motion of manipulator can be written as follows:

$$\boldsymbol{f}_c^c = \boldsymbol{W}_c(\boldsymbol{q})\ddot{\boldsymbol{r}} + \boldsymbol{\eta}_c(\boldsymbol{q},\dot{\boldsymbol{q}}) + \boldsymbol{f}^c \quad (9)$$

where $\boldsymbol{W}_c(\boldsymbol{q}) \in \Re^{m\times m}$ is the inertia matrix; $\boldsymbol{\eta}_c(\boldsymbol{q},\dot{\boldsymbol{q}}) \in \Re^m$ is the nonlinear force vector including Coriolis, centrifugal and gravitational forces in $\boldsymbol{\Sigma}^c$.

The control problem for the system (9) is to choose proper input forces to cause the end-effector to execute a desired task which can be specified either as a position tracking or as the problem of obtaining a desired contact force.

3. CONTROLLER DESIGN

When the robot manipulator is commanded to exert desired force to the normal direction of the surface while moving to the tangential direction. By defining the constraint frame at the end-effector, description of such task can be simplified.

3.1 Hybrid Impedance Control in Constraint Frame

Based on [1, 4] and the previous analysis, the target impedance can be represented in $\boldsymbol{\Sigma}^c$ as follows

$$\begin{aligned}\boldsymbol{M}_d(\ddot{\boldsymbol{r}} - \boldsymbol{S}\ddot{\boldsymbol{r}}_d) &+ \boldsymbol{B}_d(\dot{\boldsymbol{r}} - \boldsymbol{S}\dot{\boldsymbol{r}}_d) + \boldsymbol{K}_d\boldsymbol{S}(\boldsymbol{r} - \boldsymbol{r}_d)\\ &= \alpha(\bar{\boldsymbol{S}}\boldsymbol{f}_d^c - \boldsymbol{f}^c),\end{aligned} \quad (10)$$

where $\boldsymbol{M}_d$, $\boldsymbol{B}_d$, $\boldsymbol{K}_d \in \Re^{3\times3}$ are desired inertia, damping coefficient, stiffness matrices, respectively. In (10), $\bar{\boldsymbol{S}} = \boldsymbol{I} - \boldsymbol{S}$ and the compliance selection matrix $\boldsymbol{S} \in \Re^{3\times3}$ and λ_d, $\lambda \in \Re$ are expressed by

$$\boldsymbol{S} = \begin{bmatrix}1&0&0\\0&1&0\\0&0&1-\sigma(\lambda)\end{bmatrix},\ \boldsymbol{f}_d^c = \begin{bmatrix}0\\0\\\lambda_d\end{bmatrix},\ \boldsymbol{f}^c = \begin{bmatrix}0\\0\\\lambda\end{bmatrix} \quad (11)$$

where $\sigma(\cdot)$ denotes the unit step function and λ_d, $\lambda \in \Re$ are the desired and reaction contact force along $\hat{\boldsymbol{n}}$.

The command acceleration $\ddot{\boldsymbol{r}}_c$ in $\boldsymbol{\Sigma}^c$ can be given by

$$\begin{aligned}\ddot{\boldsymbol{r}}_c = \boldsymbol{S}\ddot{\boldsymbol{r}}_d + \boldsymbol{M}_d^{-1}[&\boldsymbol{B}_d(\boldsymbol{S}\dot{\boldsymbol{r}}_d - \dot{\boldsymbol{r}}) + \boldsymbol{K}_d\boldsymbol{S}(\boldsymbol{r}_d - \boldsymbol{r})\\ &+\alpha(\bar{\boldsymbol{S}}\boldsymbol{f}_d^c - \boldsymbol{f}^c)].\end{aligned} \quad (12)$$

The position error should be converted from the reference frame as follows:

$$\boldsymbol{r}_d - \boldsymbol{r} = \boldsymbol{R}(\boldsymbol{x}_d - \boldsymbol{x}). \quad (13)$$

Usually, the desired impedance parameters are given as diagonal matrices in the constraint frame. And also, to make stable contact with environment, the desired inertia should be larger than the real end-effector inertia[9]. However, it is difficult to choose the larger inertia gain for overall configuration. A possible method is to set the desired inertia as $\boldsymbol{M}_d = \boldsymbol{W}_c(\boldsymbol{q})$. With this choice, joint torque can be utilized more efficiently and the passivity can be conserved[7, 8]. In this case, however, the desired impedance is inertially coupled and the force feedback term is disappear in control input. So, the scaling factor α is inserted in (10) and it can be used to scale the desired inertia for all direction. For stable contact with the environment, α should be less than one. This yields the large inertia gain for the force control mode, effectively.

From (9), (12) with $\boldsymbol{M}_d = \boldsymbol{W}_c(\boldsymbol{q})$, the input force $\boldsymbol{f}_c^c$ is

$$\begin{aligned}\boldsymbol{f}_c^c = \boldsymbol{W}_c(\boldsymbol{q})\boldsymbol{S}\ddot{\boldsymbol{r}}_d + \boldsymbol{B}_d(\boldsymbol{S}\dot{\boldsymbol{r}}_d - \dot{\boldsymbol{r}}) + \boldsymbol{K}_d\boldsymbol{S}\boldsymbol{R}(\boldsymbol{x}_d - \boldsymbol{x})\\ +\alpha(\bar{\boldsymbol{S}}\boldsymbol{f}_d^c - \boldsymbol{f}^c) + \boldsymbol{\eta}(\boldsymbol{q},\dot{\boldsymbol{q}}) + \boldsymbol{f}^c.\end{aligned} \quad (14)$$

As shown in (14), the controller requires much computational efforts and precise information of robot manipulator. Practically, it is difficult to identify dynamic parameters exactly. In next section, the disturbance observer technique will be used to simplify the computation and to improve the robustness.

3.2 Disturbance Observer

Robustness and computational efficiency of the disturbance observer have been demonstrated by several experiments[3, 6]. Various types of the disturbance observer have been proposed. In this study, we use a disturbance observer in the constraint frame[5] which can be shown in Fig. 3. Where $\hat{\boldsymbol{W}}_c(\boldsymbol{q})$ is the estimate of $\boldsymbol{W}_c(\boldsymbol{q})$ and $\boldsymbol{Q}(s)$ is the low-pass filter. By the abuse of notation, the following closed loop equation can be obtained.

$$\boldsymbol{f}_{ref} = \hat{\boldsymbol{W}}_c\ddot{\boldsymbol{r}} + \boldsymbol{f}^c + (\boldsymbol{I} - \boldsymbol{Q}(s))\boldsymbol{f}_{dist} \quad (15)$$

where the disturbance force $\boldsymbol{f}_{dist}$ is

$$\boldsymbol{f}_{dist} = \boldsymbol{f}_c^c - \hat{\boldsymbol{W}}_c(\boldsymbol{q})\ddot{\boldsymbol{r}} - \boldsymbol{f}^c \quad (16)$$

$$= [\boldsymbol{W}_c(\boldsymbol{q}) - \hat{\boldsymbol{W}}_c(\boldsymbol{q})]\ddot{\boldsymbol{r}} + \boldsymbol{\eta}(\boldsymbol{q},\dot{\boldsymbol{q}}). \quad (17)$$

In (15), if $\boldsymbol{Q}(s)$ is close to $\boldsymbol{I}$ in low frequency region, we can reshape dynamics of the manipulator like the nominal system. However, $\boldsymbol{Q}(s) \approx \boldsymbol{0}$ in high frequency region for noise rejection. Moreover, if $\boldsymbol{f}_{ref}$ is given by

$$\begin{aligned}\boldsymbol{f}_{ref} = \hat{\boldsymbol{W}}_c(\boldsymbol{q})\boldsymbol{S}\ddot{\boldsymbol{r}}_d + \boldsymbol{B}_d(\boldsymbol{S}\dot{\boldsymbol{r}}_d - \dot{\boldsymbol{r}}) + \boldsymbol{K}_d\boldsymbol{S}\boldsymbol{R}(\boldsymbol{x}_d - \boldsymbol{x})\\ +\alpha(\bar{\boldsymbol{S}}\boldsymbol{f}_d^c - \boldsymbol{f}^c) + \boldsymbol{f}^c,\end{aligned} \quad (18)$$

then the target impedance can be achieved.

4. SIMULATION

Two degrees of freedom planar manipulator is used in the simulation study. 500Hz of the sampling frequency is assumed and the numerical integration step is taken 100 times faster than this frequency to emulate the continuous system. The manipulator and environment, $\phi(\boldsymbol{x}) = 5x + y - 2$ are shown in Fig. 4. The environment is considered as the stiffness model, *i.e.*, $\lambda = k_e\,\delta$ and $k_e = 100.0\,\mathrm{N/mm}$. Link lengths are $l_1 = 0.35$, $l_2 = 0.2\mathrm{m}$, respectively. Additionally, actuator saturation, *i.e.*, $\tau_{1,max} = 45$, $\tau_{2,max} = 15\mathrm{Nm}$, is considered. Initially, the robot is not in contact with the environment. The robot is commanded to follow the straight line trajectory denoted as dashed line in Fig. 4. When the robot contacts with the environment, 20N of desired force is required to the normal direction of the environment and for the tangential direction, the end-effector follows the trajectory. the target impedance parameters are given by

$$\alpha = 0.8,\ \boldsymbol{B}_{pd} = 40\boldsymbol{I},\ \boldsymbol{B}_{fd} = 100\boldsymbol{I} \text{ and } \boldsymbol{K}_d = 400\boldsymbol{I}.$$

Two cases study are considered. The first case is that perfect modeling is assumed and (14) is used as the controller. The other case is that the modeling error is considered and (18) with the disturbance observer is employed as the control law.

$\boldsymbol{Q}$-filter of the disturbance observer in the second case is given by

$$\boldsymbol{Q} = \frac{a^2}{(s+a)^2}\boldsymbol{I}. \tag{19}$$

Cut-off frequency of $\boldsymbol{Q}(s)$ is about 60Hz and discretized by the bilinear transformation[3]. The simulation results are shown in Fig. 5 and Fig. 6. Fig. 5(a) shows almost perfect position tracking performance. Although the tracking error of the second case (refer to Fig. 6(a)) shows somewhat large because of the modeling error, it should be noted that without disturbance observer, unacceptable performance can be observered in this case.

During the transition phase and force control mode, almost the same results can be obtained as shown in Fig. 5(b) and Fig. 6(b). In the second case, however, command torque shows noisy signal. The reason is the numerical derivative effect in the disturbance observer. By choosing smaller cut-off frequency in $\boldsymbol{Q}$-filter, this effect can be reduced. However, it affects on the system performance. In both cases, No actuator saturation can be observed.

Oscillatory behavior of the force trajectory can be reduced by choosing smaller value of α, however, larger input torques are required in this case.

5. CONCLUSION

In this paper, a new description of the hybrid impedance control method was derived for general task execution. The target impedances were expressed in the constraint frame and disturbance observer is used to reduce the computational efforts and to improve the robustness. It was noted that to make a stable contact with high stiff environment, the desired inertia matrix in the target impedances should be larger than that of real robot manipulator. The performance of the proposed controller were verified by simulational study.

REFERENCES

[1] R. J. Anderson and M. W. Spong, "Hybrid Impedance Control of Robotic Manipulators," *IEEE J. of Robotics and Automation*, vol. 4, No. 5, pp. 549–556, Oct., 1988

[2] N. Hogan, "Impedance Control; An Approach to Manipulation: Part I–III," *Trans. ASME J. of Dyn. Syst., Meas. and Contr.*, vol. 107, pp. 1–24, Mar., 1985

[3] H. S. Lee, *Robust Digital Tracking Controllers for High-Speed/High-Accuracy Positioning Systems,* Ph.D. Dissertation, Mech. Eng., U.C. Berkeley, 1994

[4] G. J. Liu and A. A. Goldenberg, "Robust Hybrid Impedance Control of Robot Manipulators," *Proc. of IEEE Int. Conf. on Robotics and Automation*, pp. 287–292, 1991

[5] K. Kaneko, K. Komoriya, K. Ohnishi and K. Tanie, "Manipulator Control based on a Disturbance Observer in the Operational Space," *Proc. of IEEE Int. Conf. on Robotics and Automation*, pp. 902–909, 1994

[6] M. Nakano, K. Ohnishi and K. Miyachi, "A Robust Decentralized Joint Control Based on Interference Estimation," *Proc. of IEEE Int. Conf. on Robotics and Automation*, pp. 326–331, 1987

[7] W. S. Newman and M. E. Dohring, "Augmented Impedance Control: An Approach to Compliant Control of Kinematically Redundant Manipulators," *Proc. of IEEE Int. Conf. on Robotics and Automation*, pp. 30–35, 1991

[8] W. S. Newman, "Stability and Performance Limits of Interaction Controllers," *Trans. ASME J. of Dyn. Syst., Meas. and Contr.*, vol. 114, pp. 563–570, Dec., 1992

[9] R. A. Volpe, *Real and Artificial Forces in the Control of Manipulators: Theory and Experiments,* Ph.D. Dissertation, Carnegie Mellon University, 1990

[10] T. Yoshikawa, "Dynamic Hybrid Position/Force Control of Robot Manipulators–Description of Hand Constraints and Calculation of Joint Driving Force," *IEEE J. of Robotics and Automation*, vol. RA-3, No. 5, pp. 386–392, Oct., 1987

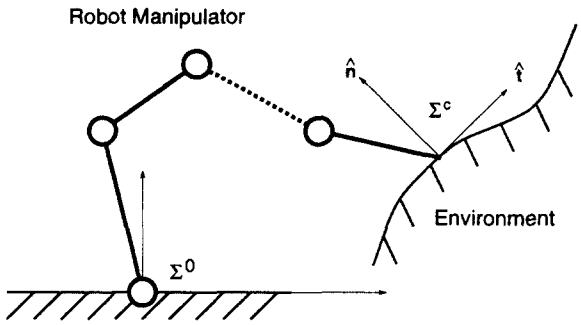

Fig. 1. Constrained arm and environment

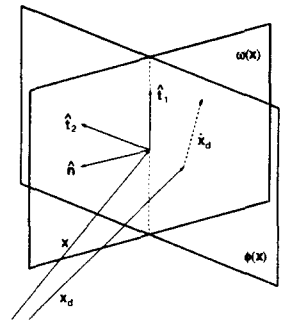

Fig. 2. Constraint frame

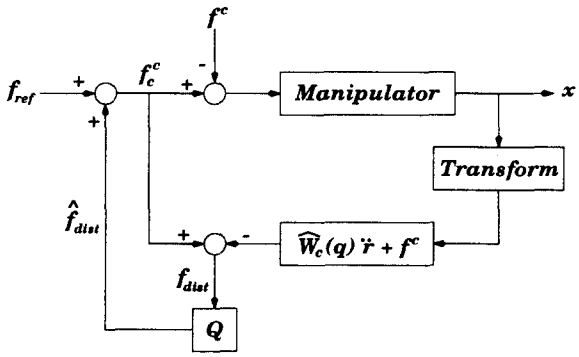

Fig. 3. Disturbance observer in constraint frame

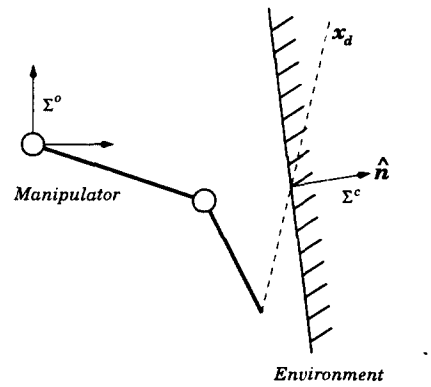

Fig. 4. Two–link planar manipulator and environment

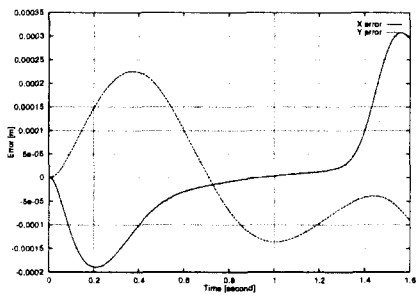

(a) position error

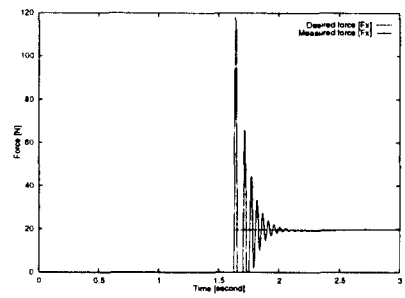

(b) force profile

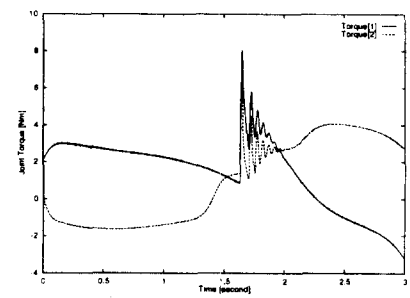

(c) torque profile

Fig. 5. Performance of ideal case HIC

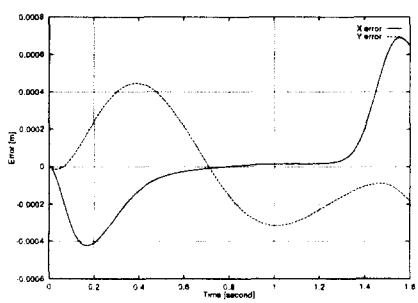

(a) position error

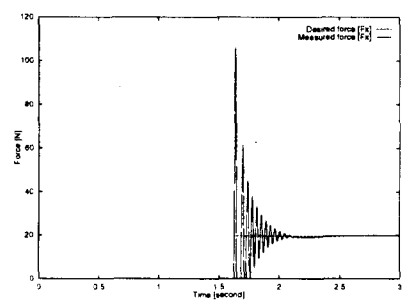

(b) force profile

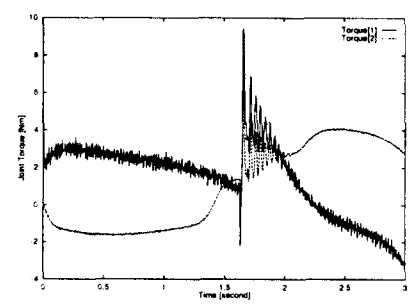

(c) torque profile

Fig. 6. Performance of HIC with disturbance observer